# ICUD-0433 Comparison of manhole hydraulics using PIV and different RANS model

M.N.A. Beg[1], R. F. Carvalho[1], J. Leandro[2], S. Tait[3], A. Schellart[3], W. Brevis

1 *Department of Civil Engineering, University of Coimbra, Coimbra, Portugal*
2 *Hydrology and River Basin Management, Technical University of Munich, Munich, Germany*
3 *Department of Civil and Structural Engineering, University of Sheffield, Sheffield, UK*

## Summary

Flows in manholes are complex and may include retardation, acceleration and rotation, however, how these complex 3D flow patterns could affect flow quantity and quality in the wider network is as yet unknown. In this work, 2D3C stereo Particle Image Velocimetry (PIV) measurements are made for the first time in a surcharged scaled circular manhole; using Laser light sheet to illuminate a 2D plane in the manhole and two cameras simultaneously to record the flow field from two different angles. A CFD model in OpenFOAM® using four different Reynolds Averaged Navier Stokes (RANS) turbulence modelling is constructed to represent flows in the manhole. Velocity profiles from the models are compared.

## Keywords

manhole, stereo PIV, RANS model, openFOAM®

## Introduction

Manholes are one of the most common features of an urban drainage network. They are located at changes in slope and orientation of the sewer pipes, as well as at regular intervals along the pipes. The flow pattern in a manhole is complex and involves several hydraulic phenomena such as e.g. contraction, expansion, rotation, air intrusion. These flow phenomena control the head loss, transport and dispersion of solute and suspended materials in the manhole structure. PIV measurement can provide a good representation of the complex velocity field of a manhole. Previously Lau (2008) studied two dimensional PIV in a surcharged scaled manhole. Attempt to measure stereo PIV data in a scaled manhole is however new and has not been done before. Several researchers studied surcharged manholes using CFD models. Use of different RANS modelling approach like RNG k-ε model (Lau et al., 2007), Realizable k-ε (Stovin et al., 2013), k-ω model (Djordjević et al., 2013) have been reported. Not much research has been done on how these flow patterns could affect flow quantity and quality in the wider piped network. In the current work, the flow phenomena of a scaled manhole is measured by stereo Particle Image Velocimetry (PIV) and modelled numerically using OpenFOAM® CFD tools. Four different RANS models i.e. RNG k-ε, Realizable k-ε, k-ω SST and Launder-Reece-Rodi (LRR) were simulated and the differences in flow structures among them were compared and discussed.

## Methods and Materials

### Experimental model

The experimental facility installed at the hydraulic laboratory of University of Sheffield used in this work consists of a transparent Perspex circular scaled manhole, linked to a flooding rig at its top, having an inner diameter of 235 mm and connected with a 75 mm inlet-outlet pipe. The setup

represents a real scale manhole as a Froude ratio of 1:6. Both pipes are co-axial and the pipe axis passes through the centre of the manhole vertical axis (Fig. 1). Two valves located at the inlet and outlet are used to control the inflow and water depth in the manhole respectively. The inflow can be monitored using an electromagnetic flow meter. The ratio between the manhole diameters to inlet pipe diameters (Φm/Φp) is 3.13. Two pressure sensors were installed at the inlet and outlet pipes at a distance of 230 mm and 400 mm respectively. They can measure piezometric pressures for both free surface and pressure flow conditions.

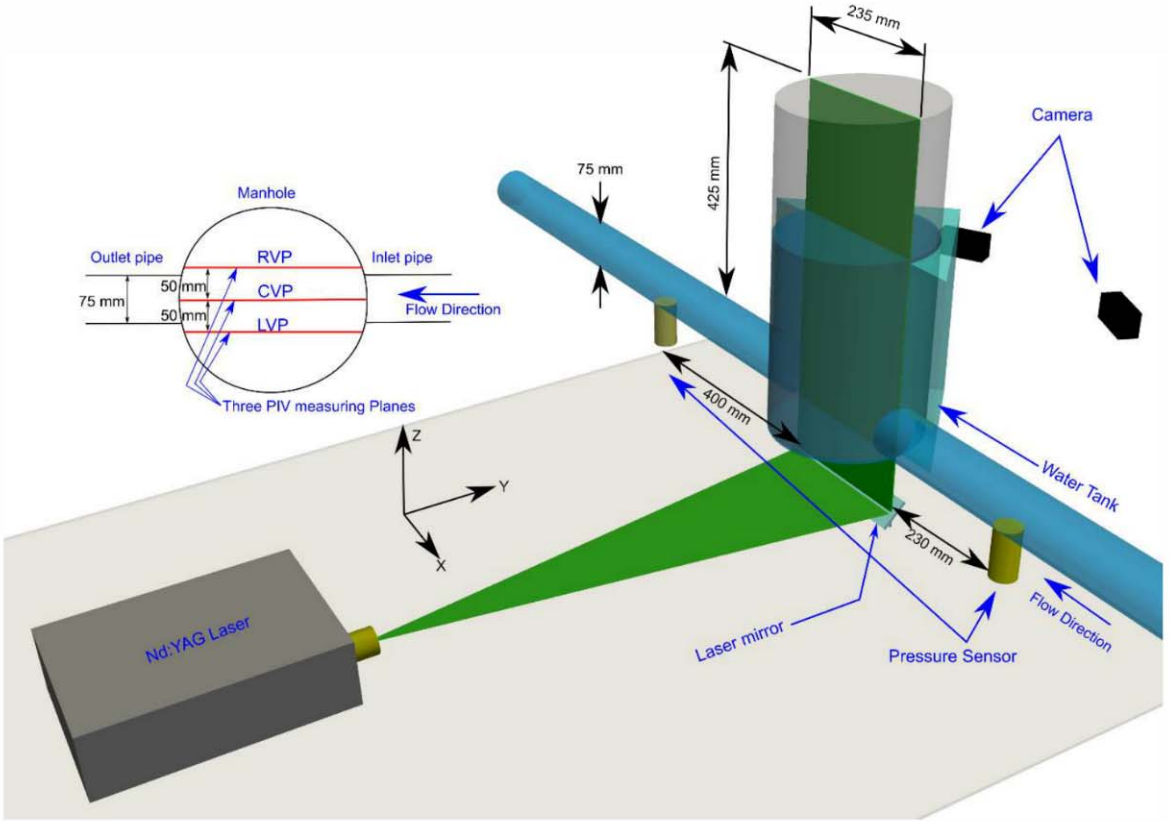


***Fig. 1.*** *Showing experimental setup for 2D3C stereo PIV measurement at the manhole*

**PIV measurement**

A stereo PIV measurement setup has been recently installed at the hydraulic laboratory. The setup consists of two Dantec FlowSense EO 2M cameras and a Nd:YAG pulsed laser was installed at two sides of the scaled manhole. Resolution of each camera is 1600x1200 pixels (Fig. 1). The two cameras were set at the same distance from the manhole making more than 45° angle at the vertical centre of the measuring plane. To reduce parallax error due to the curved manhole wall, a transparent acrylic tank was constructed around it and filled with water, keeping flat surfaces parallel to both camera lenses. The laser was sent from the bottom of the acrylic manhole as a laser sheet with the help of a laser mirror set at 45° with the horizontal direction.

Conventional 2D PIV can give the velocity vectors perpendicular to the camera direction only, which is typically parallel to the laser sheet (known as in plane velocity). But use of two cameras can give the reading of the third component of the velocity vector (known as out of plane velocity) with proper regeneration of the 2D velocities from each camera images; provided that proper calibration is done beforehand. In this work, both cameras were calibrated using standard calibration plates at two different positions so that stereo projection of the velocity vectors is possible. In this way, each calibration image sets becomes a group of four calibration images, taken from two cameras keeping the calibration plate at two different positions.

The cameras are capable to take 8 bit image pairs at very fast rate. Initial inspection showed that the measurement zone has two different distinctive velocity characteristics; one part of the measuring plane that is in line with the inlet outlet pipe has very fast jet flow, in the range of 1 m/s and the rest part is the recirculation zone have velocity magnitude in the range of few centimetres per second. For these two distinctive two characteristic velocity zones, data were taken at different time intervals ranging from 250 ms to 4000 ms; so that velocities of both fast and slow moving particles can recorded with good accuracy.

For seeding, 100 µm polyamide 12 particles were chosen. The density of this particle is very close to water (1.01 kg/m$^3$). The particles were kept in a seeding tank with continuous circulation so that they remain in suspension. The seeds were injected from the seeding tank at a constant rate from the upstream of the inlet pipe. The seeding rate was chosen by checking the PIV images on the monitor in a way so that at least 5 particles remains in a chosen interrogation window at all the time.

Measurements were taken at the manhole with combinations of different inflow and surcharge conditions. For each inflow and surcharge combinations, data was recorded at three vertical planes; one passing through the central axis of the inlet-outlet pipe and the other two at 50 mm offset from it (see Fig. 1). Each data set was measured for five minutes, at a rate of 8 pair of images per second, totalling 2400 pairs of images.

The data was analysed using Dantec Dynamics' commercial software DynamicStudio v3.31. The collected data was pre-processed after masking the area of interest. The fluid velocity was calculated using cross correlation technique. Median correction post processing was applied to get rid of the erroneous vectors.

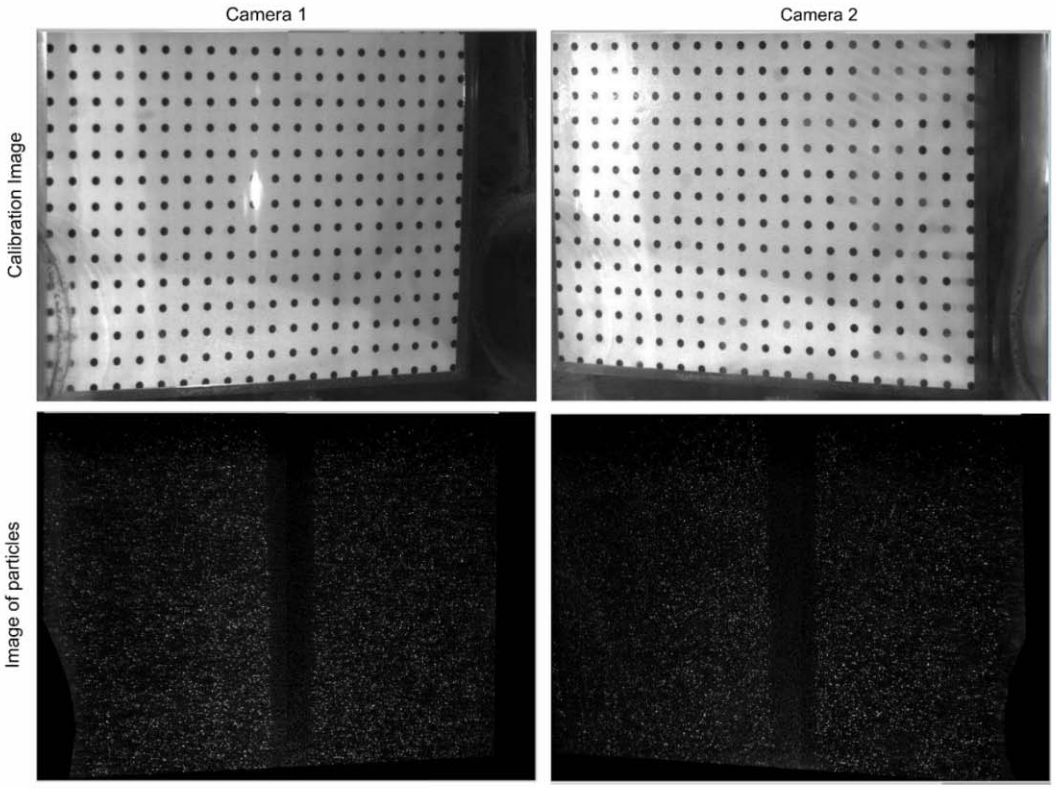


***Fig. 2.*** *Calibration images and particle images from two cameras at two different angles*

Due to the resolution and positioning laboratory setup, neither of the cameras were able to cover the whole manhole height. Emphasis was given to the incoming jet to see how the jet velocity is distributed over the manhole. Hence the data was recorded covering the lower zone of the

manhole; from the manhole bottom until the height of 150 mm of the manhole; which is two times of the inlet-outlet pipe diameter.

**Numerical model**

The numerical model aims to replicate the manhole hydraulics with the experimental model scenario. The open source CFD model tool OpenFOAM® was used in this work. The solver interFoam is selected as it can predict the free-surface flow for sharp interfaces and velocity patterns. This solver uses a single set of Navier-Stokes equations where the velocity is shared by both phases and a Volume of Fluid (VOF) method (Hirt and Nichols, 1981) capture the free-surface position. The length of the inlet pipe was kept 1m (more than 13 times the diameter) and the outlet pipe was kept as 400mm, which is until the position of the first pressure sensor at the downstream of the manhole (Fig. 3). The computational mesh for the simulation was prepared with hexahedral Cartesian mesh using *cfMesh* (Juretić, 2015). The interior and the boundary mesh sizes were kept as 4 mm and 1 mm respectively. One particular manhole flow condition was chosen from the PIV experiments at which the inflow at the manhole was 3.98 l/s and the water depth at the manhole centre was 310 mm. The wall boundary meshes were further refined considering initial simulation results, keeping the y+ value around 5.

The model utilizes three open boundaries; i.e. *inlet*, *outlet* and *atmosphere* (Fig. 3b). The inlet boundary conditions were prescribed as fixed velocity/discharge. The outlet boundary conditions were prescribed as fixed pressure boundaries corresponding to different water column pressure heads measured outlet pipe pressure sensor (shown at Fig. 1). No inflow was added at the atmosphere boundary conditions. The pressure at this boundary was prescribed as equal to *atmospheric pressure* and *zeroGradient* for velocity to have free air flow if necessary. All the close boundaries were prescribed as *noSlip* conditions (i.e. zero velocity at the wall).

The mentioned condition was simulated with four different Reynolds Average Navier-Stokes (RANS) turbulence modelling approaches; namely: RNG k-ε model, Realizable k-ε model, k-ω SST model and Launder-Reece-Rodi (LRR) model. The inlet turbulent boundary conditions $k$, $\varepsilon$, $R$ and $\nu_t$ were calculated using the equations in FLUENT manual (ANSYS Inc, 2013), considering medium turbulence at the manhole.

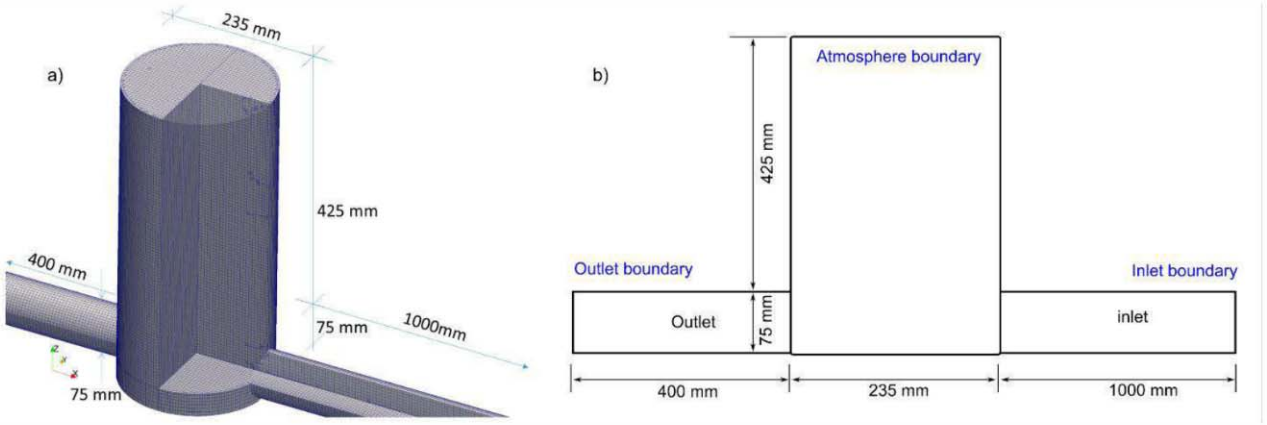


***Fig. 3.*** *Numerical model mesh and boundary locations*

The model was ready to run after the boundary setup. During the simulations, adjustableRunTime was used keeping maximum CFL number to 0.8. Cluster computing system at the University of Coimbra was used to run the simulations using MPI mode. Each simulation was run for 65 seconds. The first 60 seconds were required to reach steady state condition and the results of the last 5 seconds were saved at an interval of 0.05 seconds as 101 time steps. All the numerical analysis were made using averaged data of these mentioned time step results.

## Results and Discussion

The velocity comparison from all the four above described numerical models were checked. Fig. 4 shows the velocity vectors at the vertical and the horizontal planes passing through the inlet pipe axis.

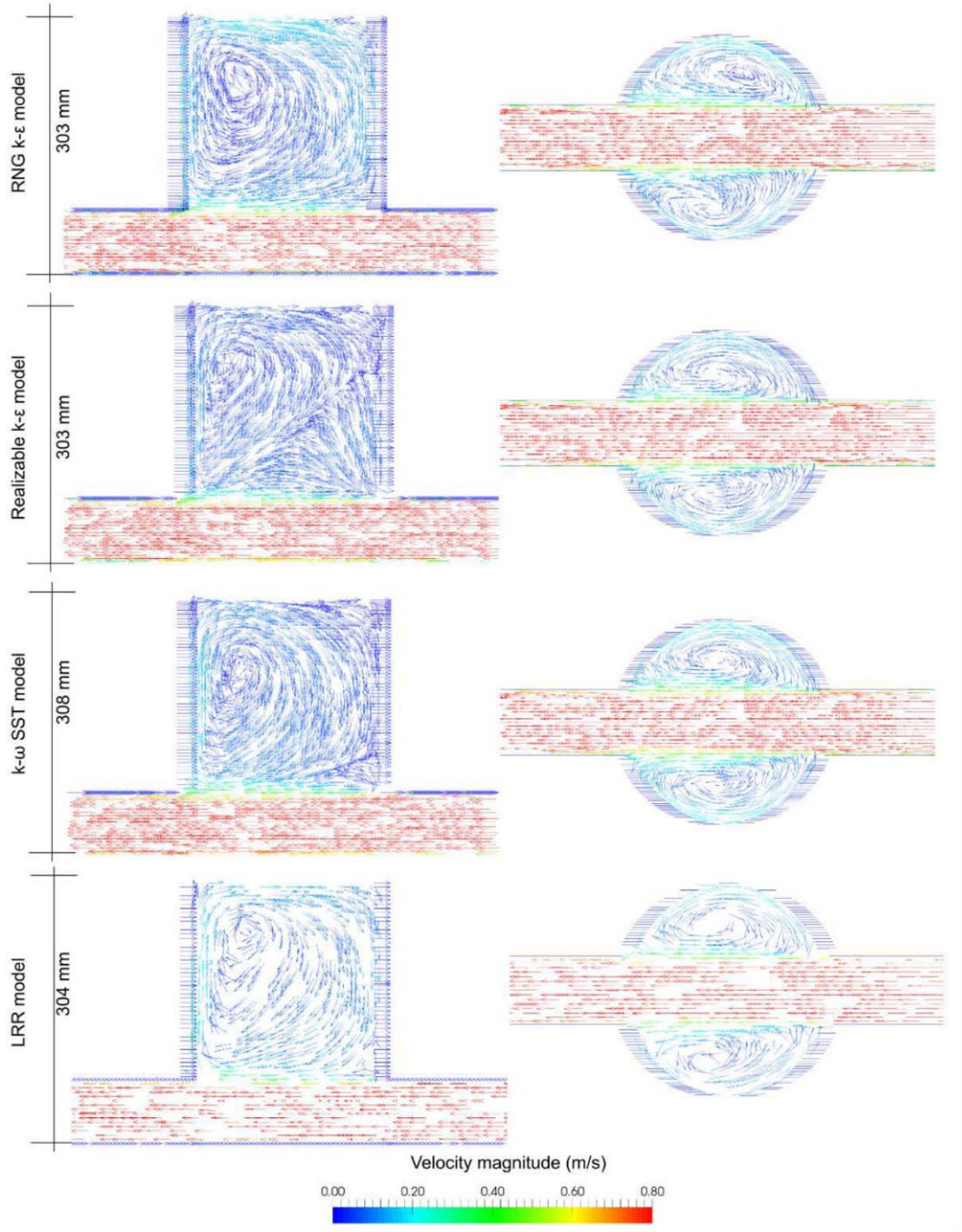


***Fig. 4.*** *Velocity fields from all the four models. Vertical centre at is shown at left panel and horizontal centre is shown at right panel. The flow direction is from right to left.*

From the velocity comparisons it can be seen that the velocity field is divided in two zones. The first zone is the high velocity zone near the inlet-outlet pipe axis. All four models represent this zone quite similarly. The second zone is the recirculation zone, where the velocity is much lower than the jet. The velocity structure at this zone is changed in different models. The velocity comparison at the vertical plane shows different size and locations of the vertical vortex. The horizontal sections of the model results also form the vortex locations differently. The depth of water is also found

slightly at different models. The calculation of the depth of water was found highest at LRR model which was 308 mm. RNG k-ε and Realizable k-ε model showed the same water depth in the manhole centre, which was 303 mm. k-ω SST model showed somewhat in the middle, 304 mm.

The processed PIV velocity data were compared with velocity data of the manhole model. The PIV measurement was taken at central vertical plane (CVP) along with the left vertical plane (LVP) and right vertical plane (RVP); of which CVP did not have much out of the plane velocity component ($V_z$). To compare with all the three velocity components, PIV data is compared at the left vertical plane of the manhole (Fig. 5).

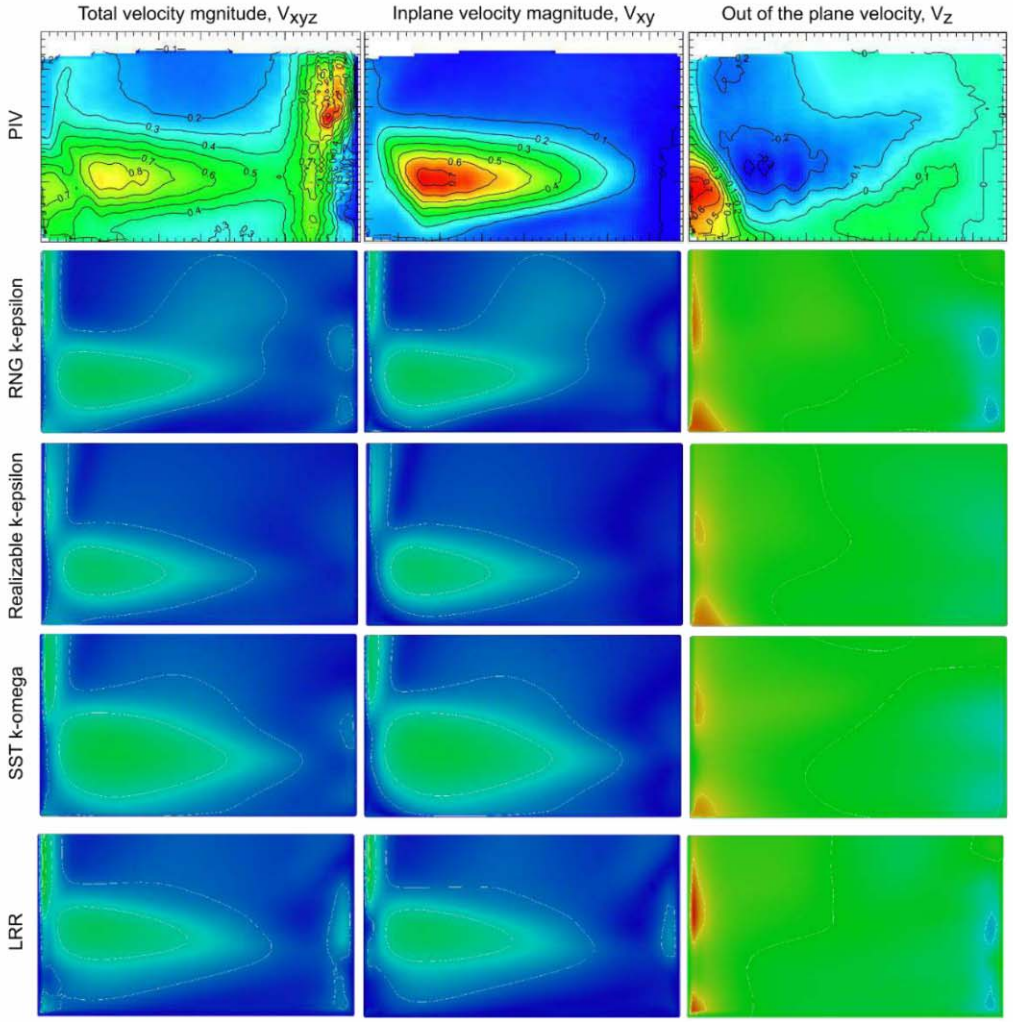


***Fig. 5.*** *Comparison of the velocity from the numerical models and PIV measurement at the LVP of the manhole. The flow direction is from right to the left*

From Fig. 5, it can be seen that in the PIV measurement, the spread of the inlet jet velocity zone is much more compared to any of the above mentioned model.

When comparing the turbulent viscosity among the models, RNG k-ε model was found showing the lowest turbulent viscosity ($\nu_t$) among all the results (Fig.6). However, in Realizable k-ε model, very high $\nu$t value can be seen at the mid-section of the inlet pipe, which is absent in the other three models.

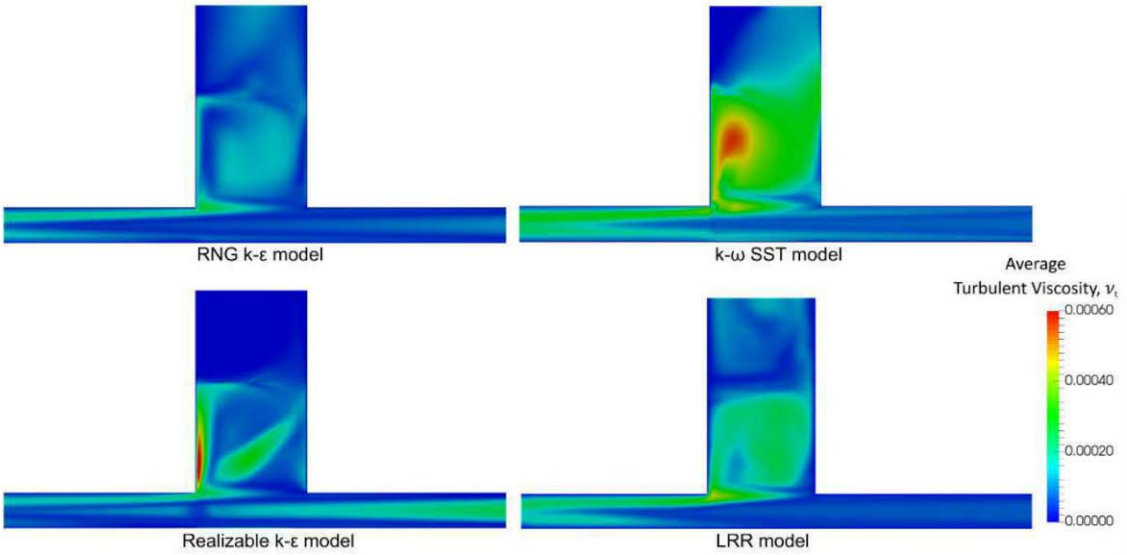


***Fig. 6.*** *Variation of turbulent viscosity at the longitudinal section of the manhole*

The pressure distribution in the model can be seen from Fig. 7, which shows the hydraulic grade line (HGL) of the manhole and throughout the length of inlet-outlet pipe. All distances are measured from the manhole centre and the inlet and outlet pipe is connected at distance of 0.1175 m and -0.1175 m respectively. The HGL in between these two distances also represents free surface water level inside the manhole. The circle markers represent average recorded pressure during the experimental measurement using pressure sensors. The left marker shows the pressure at the outlet pipe, which was used to generate boundary condition of the numerical models.

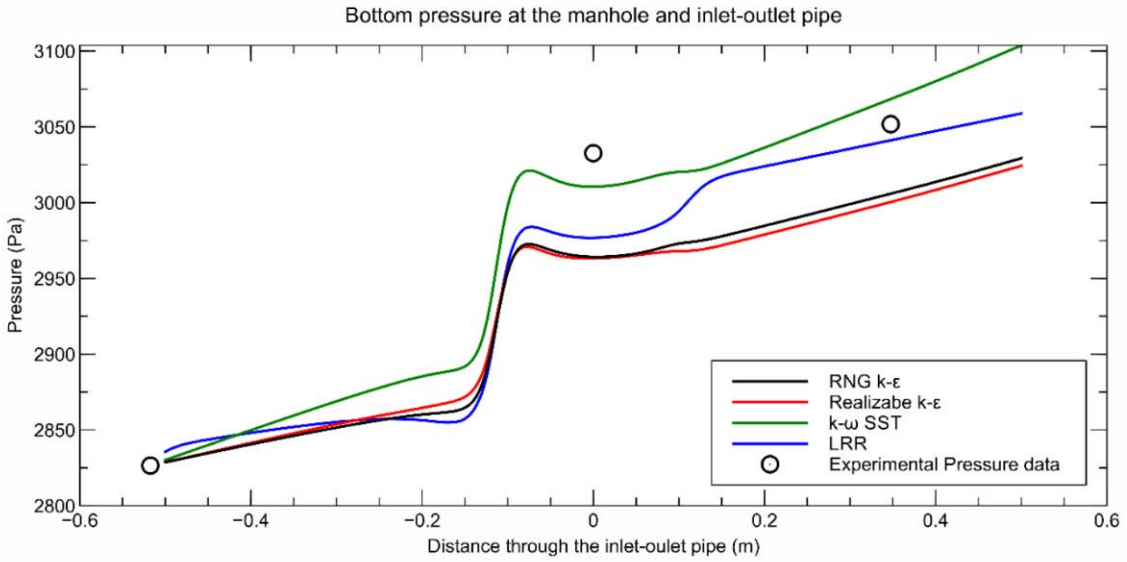


***Fig. 7.*** *Pressure comparison from different models*

From Fig. 7, it can be seen that RNG k-ε and Realizable k-ε models reproduce the pressure throughout the computational domain almost similarly. However, neither of the model could represent the exact same pressure at the inlet pipe and at centre of the manhole. Although the difference is in range of few millimetres of water column head.

The coefficient of head loss ($k$) in the manhole is calculated as the ratio between head loss and the velocity head and is calculated using equation (1) (see Tab. 1).

$$k = \Delta H / \left(\frac{v^2}{2g}\right) \quad (1)$$

where, $\Delta H$ is the head loss, $v$ (= 0.89 m/s) is the average longitudinal velocity at the outlet pipe and $g$ is the acceleration due to gravity. It can be seen that all the four models showed similar head loss coefficients except the LRR model.

***Tab. 1.*** *Different values of head loss coefficient (k) at different models*

| Simulation | Pressure drop at manhole centre ΔP (Pa) | ΔH (=ΔP/9810) (m) | k (=ΔH /($v^2$/2g)) |
|---|---|---|---|
| RNG k-ε | 67.3 | 0.0069 | 0.171 |
| Realizable k-ε | 55.1 | 0.0056 | 0.140 |
| k-ω SST | 61.6 | 0.0063 | 0.156 |
| LRR | 121.4 | 0.0140 | 0.307 |

## Conclusions

In this work, two dimensional three component (2D3C) stereo PIV measurement was done on a 1:6 scaled inline manhole. The manhole to pipe diameter ratio was 3.13. The surcharge in the manhole was higher than the threshold. The condition was reproduced using CFD and four different RANS models. The velocity structures and locations of vortex centres were found different among the models. The co-efficient of head losses were also found different. From the analysis it can be apparent that each model calculates the velocity inside manhole differently. Comparison with two dimensional-three component (2D3C) stereo PIV measurement at a vertical plane offset to the central axis showed much higher velocity in comparison to the numerical models. It has been observed that the RANS models under predict the spread of incoming water jet towards the manhole perimeters than the experimental scenario. Perhaps, a Large Eddy Simulation (LES) could represent the manhole case more effectively.

## Acknowledgement

The work presented is part of the QUICS (Quantifying Uncertainty in Integrated Catchment Studies) project. This project has received funding from the European Union's Seventh Framework Programme for research, technological development and demonstration under grant agreement No. 607000.

## References

ANSYS Inc, 2013. ANSYS Fluent Theory Guide, ANSYS Inc., USA. Canonsburg, PA, USA.

Djordjević, S., Saul, A.J., Tabor, G.R., Blanksby, J., Galambos, I., Sabtu, N., Sailor, G., 2013. Experimental and numerical investigation of interactions between above and below ground drainage systems. Water Sci. Technol. 67, 535–542. doi:10.2166/wst.2012.570

Hirt, C.W., Nichols, B.D., 1981. Volume of fluid (VOF) method for the dynamics of free boundaries. J. Comput. Phys. 39, 201–225. doi:10.1016/0021-9991(81)90145-5

Juretić, F., 2015. cfMesh User Guide (v1.1). Zagreb, Croatia.

Lau, S.D., 2008. Scaling Dispersion Processes in Surcharged Manholes. Dep. Civ. Struct. Eng. Univ. Sheff. University of Sheffield, Sheffield, UK.

Lau, S.D., Stovin, V.R., Guymer, I., 2007. The prediction of solute transport in surcharged manholes using CFD. Water Sci. Technol. 55, 57–64. doi:10.2166/wst.2007.095

Stovin, V.R., Bennett, P., Guymer, I., 2013. Absence of a Hydraulic Threshold in Small-Diameter Surcharged Manholes. ASCE J. Hydraul. Eng. 139, 984–994. doi:10.1061/(ASCE)HY.1943-7900.0000758